

# RECIPROCAL SPACE MAPPING OF ZnMgY FACE-CENTRED ICOSAHEDRAL QUASICRYSTALS

V. Karpus<sup>a</sup>, S. Tumėnas<sup>a</sup>, R. Juškėnas<sup>a</sup>, J. Birch<sup>b</sup>, and F. Eriksson<sup>b</sup>

<sup>a</sup> Center for Physical Sciences and Technology, Saulėtekio 3, 10257 Vilnius, Lithuania

<sup>b</sup> Thin Film Physics, IFM, Linköping University, SE-58183 Linköping, Sweden

Email: [vytas.karpus@ftmc.lt](mailto:vytas.karpus@ftmc.lt)

Received 5 November 2024; accepted 6 November 2024

The reciprocal lattice of face-centred icosahedral ZnMgY quasicrystals was investigated using X-ray diffractometry. A large-scale planar cut of the reciprocal ZnMgY lattice was recorded making use of a PIXcel area detector. The  $\theta$ - $2\theta$  scans along the  $C_5$ ,  $C_3$  and  $C_2$  symmetry axes revealed numerous diffraction peaks with a large dynamical range of about  $10^6$ . Low structure-factor diffraction peaks, corresponding to large complementary reciprocal lattice vectors  $\mathbf{g}_\perp$  up to  $g_\perp a = 24$  (where  $a$  is the quasilattice constant), were observed, indicating a high structural quality of ZnMgY quasicrystals. A static linear phason strain was detected in one of the five investigated ZnMgY samples.

**Keywords:** quasicrystals, X-ray diffraction, reciprocal space mapping, phason strain

**PACS:** 71.23.Ft

## 1. Introduction

Quasicrystals are the focus of extensive research due to their unique atomic structure and unusual physical properties (see, e.g. Refs. [1, 2]). Their remarkable combination of both a long-range atomic order and a five-fold rotational symmetry has been confirmed experimentally by numerous X-ray diffraction (XRD) studies.

As in other solids, the diffraction peaks of quasicrystals correspond to reciprocal lattice vectors, which for the icosahedral quasicrystals are determined by the linear combination of six unit vectors of an icosahedron [3, 4]:

$$\mathbf{g} = \frac{\pi}{a}(n_1\mathbf{e}_1 + n_2\mathbf{e}_2 + n_3\mathbf{e}_3 + n_4\mathbf{e}_4 + n_5\mathbf{e}_5 + n_6\mathbf{e}_6). \quad (1)$$

Here  $a$  is the quasilattice constant,  $n_i$  are integer numbers, and  $\mathbf{e}_i$  are the unit vectors of an icosahedron (see inset to Fig. 2).

Even though the reciprocal quasicrystalline lattice (1) is discrete, it densely fills the reciprocal space. However, the reciprocal lattice nodes of quasicrystals are modulated by their structure factors.

The structure factors depend on the complementary reciprocal-lattice vectors  $\mathbf{g}_\perp$  which, in the Elser indexing scheme, are defined as

$$\mathbf{g}_\perp = \frac{\pi}{a}(-n_1\mathbf{e}_1 + n_2\mathbf{e}_2 + n_3\mathbf{e}_3 + n_3\mathbf{e}_4 + n_6\mathbf{e}_5 + n_4\mathbf{e}_6). \quad (2)$$

The structure factor of the reciprocal lattice nodes significantly decreases with the increase of  $\mathbf{g}_\perp$  modulus. Generally, this limits an observation of diffraction peaks with  $g_\perp a$  values above about 5, and conventional powder diffraction patterns of quasicrystals are comprised of a comparatively small number of diffraction peaks. With an increase of XRD instrumental resolution, low structure-factor diffraction peaks are expected to emerge, and their manifestation is revealed in high-resolution XRD studies conducted at synchrotron facilities.

Here we present the experimental results of a lab-source based XRD study. The recorded diffraction patterns of investigated ZnMgY quasicrystals confirm the dense character of the reciprocal quasicrystalline lattice, revealing the unusually low structure-factor Bragg peaks, corresponding to  $g_\perp a$  values up to about 24.

## 2. Experiment

Face-centred icosahedral ZnMgY quasicrystals, with the atomic composition  $\text{Zn}_{62}\text{Mg}_{29}\text{Y}_9$ , were grown by a liquid-encapsulated top-seeded solution growth method at Physikalisches Institut of J. W. Goethe-Universität [5, 6]. Single-grain samples with  $C_5$ ,  $C_3$  and  $C_2$  symmetry axes along the surface normal were separated by spark cutting. Five samples were investigated in the present study: two  $C_5$  samples ('Q5' and 'N5'), one  $C_3$  and two  $C_2$ . The samples were 3–8 mm in diameter and about 3 mm in thickness.

XRD studies were performed using Empyrean (*Panalytical*) and SmartLab (*Rigaku*) diffractometers, equipped with copper-anode sources of 1.8 and 9 kW, respectively. The samples were studied in reflection geometry with an estimated penetration depth of about 20  $\mu\text{m}$ . The recorded diffraction patterns were well reproducible, and  $\theta$ - $2\theta$  scans (Cu- $K_{\alpha 1}$  line) from both diffractometers displayed consistent diffraction patterns in all details across all measurements.

Reciprocal space mapping (RSM) was carried out on the Q5 sample, with the  $C_5$  axis along the surface normal, using the Empyrean diffractometer with a PIXcel area detector. Sample orientation was achieved through pole-figure measurements using a capillary lens (0.3° incident beam divergence) and a parallel plate collimator ( $\Delta 2\theta = 0.27^\circ$ ), with the detector operating in an open detector mode. The recorded pole figures (Fig. 1) clearly demonstrate a distinct perfect 5-fold symmetry and a single-grain character

of the investigated sample. The reciprocal space mapping was conducted at the diffraction plane orientation which ensured the  $C_5$ - $C_2$ - $C_5$ - $C_3$ - $C_2$ - $C_3$  axes sequence to lie within the plane, as indicated in Fig. 2. A hybrid mirror with a  $1/32^\circ$  divergence slit was used together with the PIXcel detector operating in a scanning line mode with  $\Delta 2\theta = 0.013^\circ$ . The out-of-plane resolution was estimated to be about  $1^\circ$ .

## 3. Results and discussion

### 3.1. Reciprocal space mapping

The reciprocal space map of the ZnMgY quasicrystal, presented in Fig. 2, represents the reciprocal space plane that bisects an icosahedron along its  $C_5$ - $C_2$ - $C_5$ - $C_3$ - $C_2$ - $C_3$  axes, as indicated in the inset in Fig. 2. The recorded RSM map is comprised of about 320 diffraction peaks, all of which can be successfully indexed by six integers  $n_i$  in accordance with Eq. (1).

About 51% of the peaks in the RSM, which are indicated by squares in Fig. 3(a), satisfy the face-centred icosahedral (fci) phase reflection rule, which requires that all six  $n_i$  indices should be either even or odd.

The remaining 49% of the diffraction peaks, indicated by circles in Fig. 3(a), correspond to the sets of  $n_i$  indices, which are comprised of either four even and two odd or two even and four odd indices. They satisfy the body-centred icosahedral (bci) phase reflection rule 'a sum of  $n_i$  indices should be an even number' and,

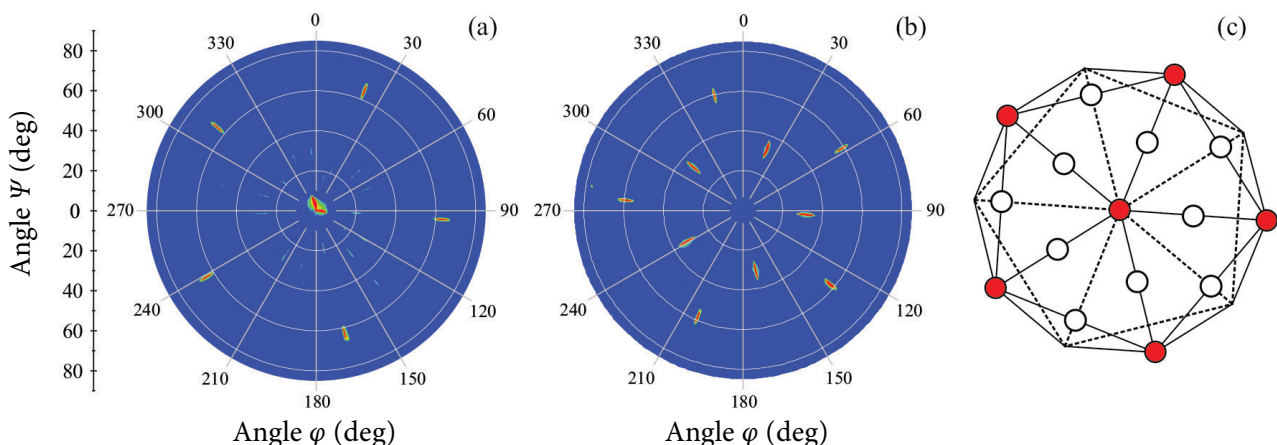


Fig. 1. Pole figures of (a) the 5-fold (422222) peak at  $2\theta = 36.6^\circ$  and (b) the 2-fold (442002) peak at  $2\theta = 38.6^\circ$ . The recorded 5-fold and 2-fold poles are indicated by full and open dots, respectively, in the schematic drawing (c).

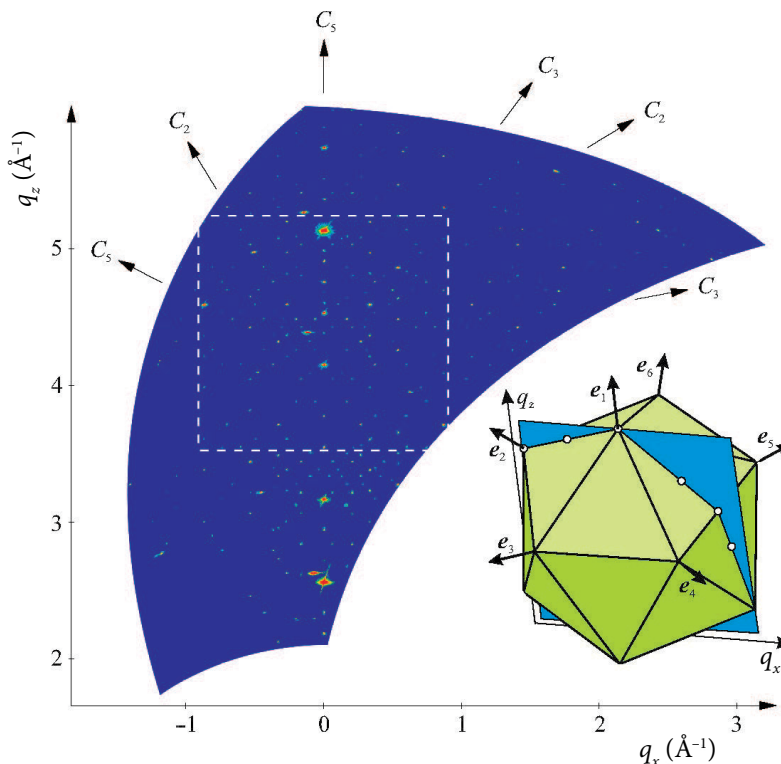


Fig. 2. ZnMgY reciprocal space map. The white-dashed square section of the map is analyzed further in Fig. 3. The inset indicates the orientation of the RSM plane with respect to an icosahedron.

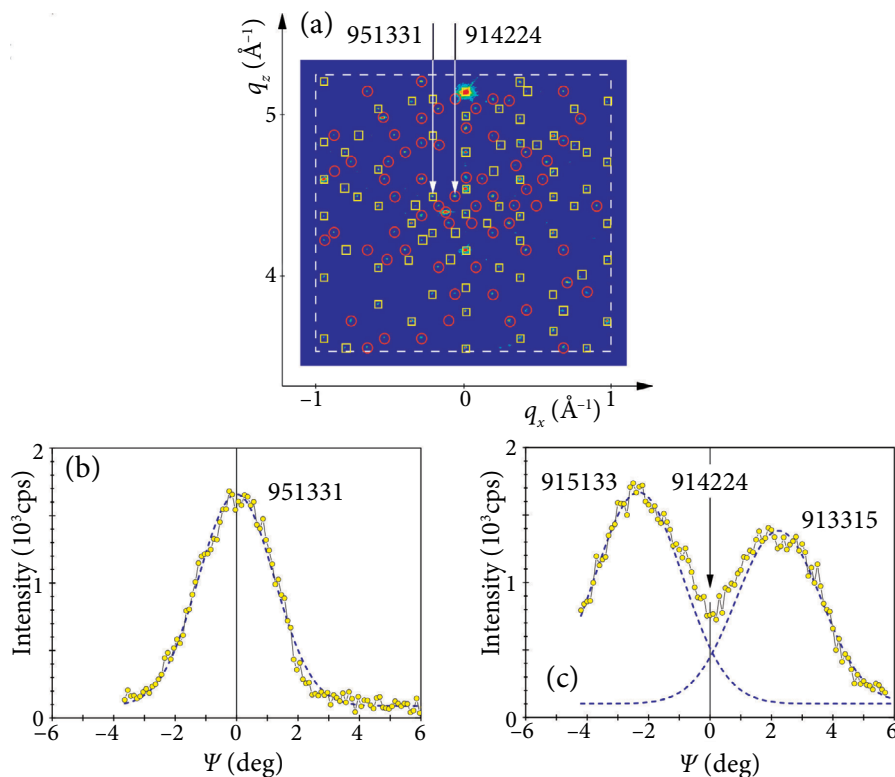


Fig. 3. (a) Section of the reciprocal space map. Diffraction peaks indicated by squares and circles correspond to the fci and ‘bci-like’ indices, respectively. (b, c) Psi-scans of the (951331) fci peak,  $(q_x, q_z) = (-0.21, 4.48) \text{ \AA}^{-1}$ , and the (914224) ‘bci-like’ peak,  $(q_x, q_z) = (-0.06, 4.48) \text{ \AA}^{-1}$ .

therefore, suggest a presumable bci phase of the investigated sample.

However, the recorded ‘bci-like’ diffraction peaks are superpositions of pairs of fci peaks. Each ‘bci-like’ diffraction peak is due to two closely positioned fci reciprocal lattice nodes, which lie slightly out of the map plane and which are mirror images of each other across the plane. They are traced in the reciprocal space map due to a comparatively low out-of-plane instrumental resolution. This can be proved by scanning the diffraction peak profiles in a direction perpendicular to the plane. The scans were carried out by varying the sample tilt angle  $\Psi$ , what approximately corresponds to a parallel shift of the RSM plane in the  $q_y$  direction. The  $\Psi$ -scans of two chosen diffraction peaks – an fci peak (951331) and a ‘bci-like’ peak (914224) – are presented in Fig. 3(b, c). As seen, the (951331) peak corresponds to a true reciprocal lattice node  $\mathbf{g}_{951331}$ , while the (914224) peak is ‘empty’, – the non-existing lattice vector  $\mathbf{g}_{914224}$  is formed by 2 fci  $\mathbf{g}$ -vectors,

$$\mathbf{g}_{914224} = 1/2 (\mathbf{g}_{915133} + \mathbf{g}_{913315}),$$

$$(914224) = 1/2 [(915133) + (913315)].$$

Consequently, all diffraction peaks recorded in the reciprocal space map (Fig. 2) confirm the face-centred icosahedral phase of the ZnMgY quasicrystal.

In what follows, we will adopt the conventional fci indexing scheme, in the framework of which the fci lattice is treated as a superstructure on a primitive icosahedral lattice. The quasilattice constant is taken as half of the fci one, and the indices of  $\mathbf{g}$ -vectors, in accordance with Eq. (1), are divided by 2. Then, all-even fci indices are reduced to sets of six integers, while all-odd indices are reduced to sets of six half integers.

### 3.2. $\theta$ - $2\theta$ diffraction

For detailed scans of the ZnMgY reciprocal lattice along the  $C_5$ ,  $C_3$  and  $C_2$  symmetry axes,  $\theta$ - $2\theta$  diffractograms were recorded in the 10–150° interval of the diffraction angle  $2\theta$ . The obtained diffractograms are comprised of numerous diffraction peaks: up to about 70 reflexes along the  $C_5$  axis, ~50 along  $C_3$  and ~30 along  $C_2$ . Figures 4 and 5(a) present a wide range  $\mathbf{q} \parallel C_5$  diffractogram and its short-range section, respectively. Successful indexing of the observed diffraction peaks allows for a determination of the quasilattice constant to be  $a = 5.19 \text{ \AA}$ .

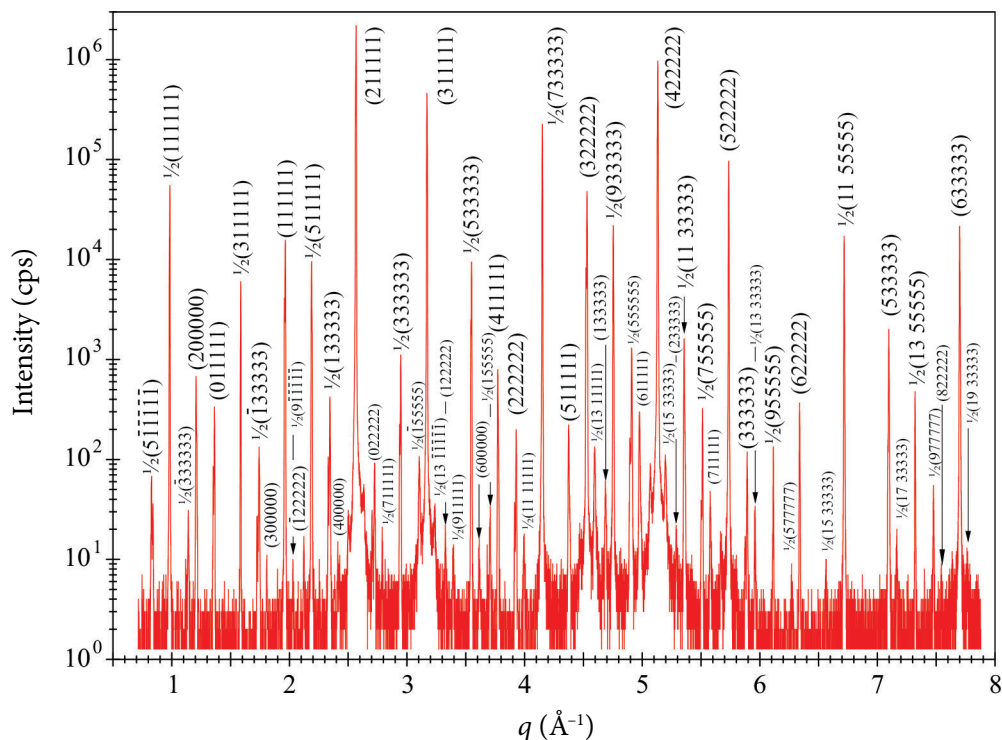


Fig. 4. The  $\theta$ - $2\theta$  diffractogram (of sample Q5) along the  $C_5$  axis.

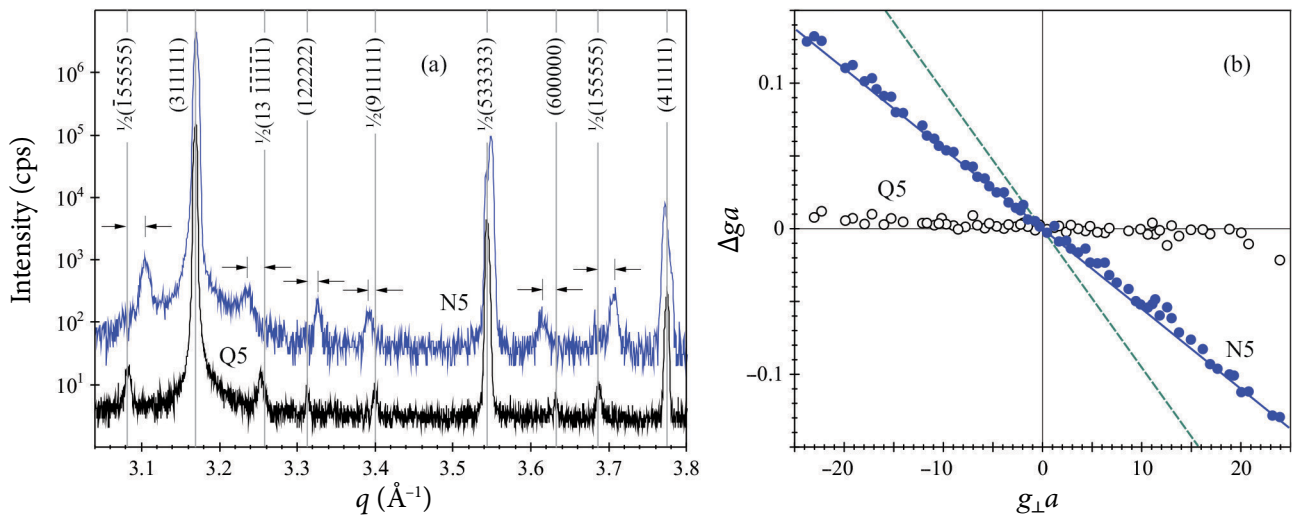


Fig. 5. (a) Short-range  $\theta$ - $2\theta$  diffractogram along the  $C_5$  axis of the ZnMgY sample Q5 with Bragg peaks at their theoretical positions (lower curve) and of the N5 sample with shifted peaks (upper curve, displaced vertically for visual clarity). (b) Dependence of the peak shifts on the complementary reciprocal lattice vector. (Open and full dots correspond to Q5 and N5 samples, respectively). A dashed line presents, for a comparison, Létoublon et al. [8] data.)

As seen from Fig. 4, the intensities of the recorded diffraction peaks cover a large dynamical range of about  $10^6$ . The intensities of the diffraction peaks in quasicrystals depend on the complementary reciprocal-lattice vector  $\mathbf{g}_\perp$ . The structure factors  $S_g$  of the reciprocal quasicrystalline lattice nodes decrease significantly with the increase of the  $\mathbf{g}_\perp$  modulus, and, as a result, a comparatively small number of diffraction peaks, with  $g_\perp a \lesssim 5$ , usually contributes to conventional powder diffractograms. The larger complementary reciprocal lattice vectors are disclosed in high-resolution synchrotron-radiation facilities XRD studies, in which, e.g. the  $g_\perp a = 11.4$  diffraction peaks were resolved for a high structural quality AlPdMn quasicrystal [7].

In the present study, Bragg peaks with very large  $g_\perp a$  values, up to 24, were resolved. In the recorded  $C_5$ ,  $C_3$  and  $C_2$  diffractograms, almost all possible diffraction peaks with  $g_\perp a < 20$  values were observed, with an exception of the (722222) peak which corresponds to a comparatively low value,  $g_\perp a = 7.94$ . The extinction is most probably due to an atomic decoration of the fci-ZnMgY quasilattice.

The low-intensity peaks  $1/2(\bar{1}55555)$  and  $1/2(13\bar{1}\bar{1}\bar{1}\bar{1}\bar{1})$ , surrounding the strong (311111) peak (see Fig. 5(a)), correspond to the  $g_\perp a = 19.13$  and 23.93 values, respectively. They are comparable with the  $g_\perp a = 17.3$  value for the fci-Zn<sub>57</sub>Mg<sub>34</sub>Y,

quasicrystals reported by Létoublon et al. [8] in the synchrotron XRD study. Since synchrotron facilities generally provide a higher instrumental resolution than conventional diffractometers, the observation of large fci-ZnMgY complementary  $\mathbf{g}_\perp$  vectors in our diffractograms is most probably due to a higher structural quality of the investigated ZnMgY samples.

The manifestation of low structure-factor reciprocal lattice nodes of fci-ZnMgY was previously indirectly revealed in the ZnMgY optical spectroscopy study [9]. Interband optical transitions occur across the pseudogaps determined by the  $\mathbf{g}$ -vectors, the Bragg planes of which are in the proximity of the Fermi surface. Along the  $C_5$  directions, these are the  $\mathbf{g}_{311111}$  vectors, corresponding to the  $\Delta_{311111} = 1.12$  eV pseudogap. The analysis of the ZnMgY optical conductivity spectrum revealed, apart from the optical transitions across the  $\Delta_{311111}$  pseudogap, a contribution of small- $S_g$  pseudogaps, estimated to be roughly 0.03–0.04 eV. As seen from Fig. 5(a), the  $\Delta_{311111}$  vectors are surrounded by weak  $1/2(\bar{1}55555)$  and  $1/2(13\bar{1}\bar{1}\bar{1}\bar{1}\bar{1})$  vectors. The ratios of their structure factors to the structure factor of  $\mathbf{g}_{311111}$  can be estimated from the square roots of the diffraction peak intensities and are about 0.01–0.02, and this agrees in order of magnitude with the estimate from optical data.

#### 4. Phason strain

Phasons are related with specific deformations of the 6-dimensional hyperlattice, from which the quasicrystalline lattice is projected [10–12]. The best-known example of a manifestation of the static linear phason strain is a shift of diffraction peaks from their theoretical positions,  $\Delta\mathbf{g} = \mathbf{g}_{\text{exper}} - \mathbf{g}_{\text{theor}}$ . The peak shifts are larger for low-intensity peaks and linearly depend on the  $\mathbf{g}_{\perp}$ -vector:

$$\Delta\mathbf{g} = b\mathbf{g}_{\perp}. \quad (3)$$

The static-phason-strain-induced shifts of diffraction peaks were observed in XRD studies of various quasicrystals. For the fci-Zn<sub>57</sub>Mg<sub>34</sub>Y<sub>9</sub> quasicrystals, the shifts were reported by Létoublon et al. [8].

Out of the five fci-ZnMgY samples investigated in the present study only one, the N5 sample, which was from a different growth batch than the other four, was subjected to the static phason strain. Figure 5(a) presents the diffractograms of N5 and Q5 samples, the surface normals of which were directed along the  $C_5$  symmetry axes. As seen, the Bragg peaks of the Q5 sample (lower curve in Fig. 5(a)) are at their expected, theoretical positions, which are indicated in the figure by vertical lines. However, the Bragg peaks of the N5 sample (upper curve

in Fig. 5(a)) are slightly shifted from the theoretical positions, and the shifts closely follow the linear dependence (3), see Fig. 5(b). The slope parameter of the linear peak shift is about  $b = -0.0055$  and indicates the phason strain to be about half of that observed by Létoublon et al. [8],  $b = -0.0095$  (dashed line in Fig. 5(b)).

We assume that the static phason strain in the N5 sample was induced by its surface layer. After the mechanical grinding (which was intended to remove a layer of about 20  $\mu\text{m}$ ) and the subsequent careful polishing of the sample, its diffraction peaks shifted to their theoretical positions, as illustrated in Fig. 6.

#### 5. Summary

Summarizing, the present XRD study of fci-ZnMgY quasicrystals, conducted using diffractometers with conventional copper-anode X-ray sources, has revealed a rich, dense structure of the reciprocal quasicrystalline lattice. The large-scale planar section of the lattice was recorded by the RSM technique. The  $\theta$ - $2\theta$  scans along the  $C_5$ ,  $C_3$  and  $C_2$  symmetry axes revealed diffraction peaks with unusually large complementary reciprocal lattice vectors up to  $\mathbf{g}_{\perp}a \approx 24$ , indicating a high structural quality of the studied ZnMgY quasicrystals. The static linear phason strain, presumably induced by

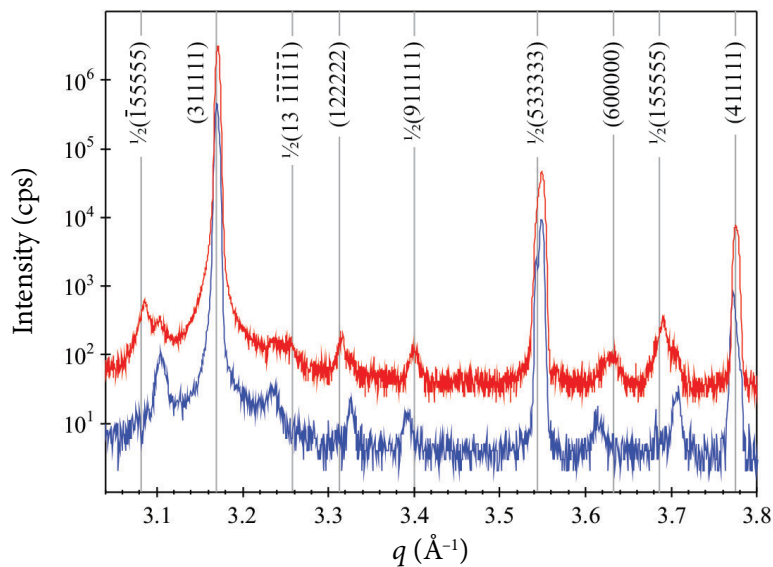


Fig. 6. Short-range  $\theta$ - $2\theta$  diffractogram along the  $C_5$  axis of the N5 sample before (lower curve) and after (upper curve, displaced vertically for visual clarity) the removal of its surface layer.

a surface layer, was detected in one of the five ZnMgY samples studied.

### Acknowledgements

The authors gratefully acknowledge the support by the Research Council of Lithuania (Grant MIP-081/2012).

We are indebted to Wolf Assmus, Lars Hultman and Simon Olsson for the growth of samples, the discussion of results and their help in XRD measurements.

### References

- [1] T. Janssen, G. Chapuis, and M. de Boissieu, *Aperiodic Crystals. From Modulated Phases to Quasicrystals* (Oxford University Press, 2007).
- [2] E. Maciá Barber, *Quasicrystals: Fundamentals and Applications* (Taylor & Francis, 2021).
- [3] V. Elser, Indexing problems in quasicrystal diffraction, *Phys. Rev. B* **32**(8), 4892–4898 (1985).
- [4] V. Elser, The diffraction pattern of projected structures, *Acta Cryst. A* **42**(1), 36–43 (1986).
- [5] A. Langsdorf and W. Assmus, Growth of large single grains of the icosahedral quasicrystal ZnMgY, *J. Cryst. Growth* **192**(1–2), 152–156 (1998).
- [6] A. Langsdorf and W. Assmus, Crystal growth of large icosahedral Zn-Mg-Y single grains by a liquid encapsulated top seeded solution growth method, *Cryst. Res. Technol.* **34**(2), 261–265 (1999).
- [7] M. Boudard, M. de Boissieu, J.P. Simon, J.F. Berar, and B. Doisneau, Phason strain in a mechanically polished Al-Pd-Mn icosahedral single quasicrystal, *Phil. Mag. Lett.* **74**(6), 429–437 (1996).
- [8] A. Létoublon, I.R. Fisher, T.J. Sato, M. de Boissieu, M. Boudard, S. Agliozzo, L. Mancini, J. Gastaldi, P.C. Canfield, A.I. Goldman, and A.-P. Tsai, Phason strain and structural perfection in the Zn–Mg–rare-earth icosahedral phases, *Mater. Sci. Eng. A* **294–296**, 127–130 (2000).
- [9] V. Karpus, S. Tuménas, A. Suchodolskis, H. Arwin, and W. Assmus, Optical spectroscopy and electronic structure of the face-centered icosahedral quasicrystals Zn-Mg-R ( $R = Y, Ho, Er$ ), *Phys. Rev. B* **88**(3), 094201 (2013).
- [10] T.C. Lubensky, J.E.S. Socolar, P.J. Steinhardt, P.A. Bancel, and P.A. Heiney, Distortions and peak broadening in quasicrystal diffraction patterns, *Phys. Rev. Lett.* **57**(12), 1440–1443 (1986).
- [11] C. Janot, L. Loreto, and R. Farinato, Special defects in quasicrystals, *Phys. Status Solidi B* **222**(1), 121–132 (2000).
- [12] M. de Boissieu, Phason modes in quasicrystals, *Phil. Mag.* **88**(13–15), 2295–2309 (2008).

## PAVIRŠIAUS CENTRUOTŲ IKOSAEDRINIŲ ZnMgY KVAZIKRISTALŲ ATVIRKŠTINĖS ERDVĖS PJŪVIAI

V. Karpus<sup>a</sup>, S. Tumėnas<sup>a</sup>, R. Juškėnas<sup>a</sup>, J. Birch<sup>b</sup>, F. Eriksson<sup>b</sup>

<sup>a</sup> *Fizinių ir technologijos mokslų centras, Vilnius, Lietuva*

<sup>b</sup> *Linšioopingo universitetas, Linšioingas, Švedija*

### Santrauka

Kvazikristalų, kaip ir įprastinių kristalų, atvirkštinė gardelė yra diskreti, nors kvazikristalinės, kitaip nei kristalinės, atvirkštinės gardelės vektoriai  $\mathbf{g}$  užlieja visą atvirkštinę erdvę, – teoriškai bet kuri kvazikristalo atvirkštinės erdvės tašką atitinka gardelės mazgas. Tačiau kvazikristalinės atvirkštinės gardelės mazgus moduliuoja struktūrinis faktorius, kurį apibrėžia antrinis, papildomas atvirkštinės gardelės vektorius  $\mathbf{g}_\perp$ . Struktūrinis faktorius greitai mažėja augant  $\mathbf{g}_\perp$  vektorių moduliui, ir dėl šios priežasties įprastines kvazikristalų difraktogramas paprastai sudaro palyginti nedidelis refleksų, atitinkančių žemas  $g_\perp a \lesssim 5$  vertes, skaičius (čia  $a$  – kvazigardelės konstanta). Didėjant XRD aparatūrinei skiriamajai gebai, kvazikristalų difraktogramos atskleidžia vis daugiau refleksų. Tai paprastai pasiekama naudojant sinchroninės spinduliuotės rentgeno spindulių šaltinius.

Šiame darbe pateikiami ZnMgY kvazikristalų rentgeno-difrakcinių tyrimų rezultatai, kurie buvo gauti naudojantis įprastiniais rentgeno spindulių šaltiniais (*Panalytical Empyrean* ir *Rigaku SmartLab* difraktometrais). Gautos difraktogramos demonstruoja turtingą, tankią kvazikristalų atvirkštinės gardelės struktūrą ir atskleidžia difrakcinius refleksus, atitinkančius neįprastai dideles antrinių atvirkštinės gardelės vektorių vertes,  $g_\perp a \approx 24$ . (Tokios  $\mathbf{g}_\perp$  vektorių vertės anksčiau buvo stebėtos tik sinchroniniuose rentgeno-difrakciniuose tyrimuose.) Kadangi įprastinių difraktometrų skiriamoji geba paprastai yra mažesnė nei sinchroninių, gauti rezultatai liudija išskirtinį tirtų ZnMgY monokvazikristalų struktūrinį tobulumą.